

Subpicosecond monolithic collidingpulse modelocked multiple quantum well lasers

Y. K. Chen, M. C. Wu, T. TanbunEk, R. A. Logan, and M. A. Chin

Citation: [Applied Physics Letters](#) **58**, 1253 (1991); doi: 10.1063/1.104327

View online: <http://dx.doi.org/10.1063/1.104327>

View Table of Contents: <http://scitation.aip.org/content/aip/journal/apl/58/12?ver=pdfcov>

Published by the [AIP Publishing](#)

Articles you may be interested in

[Chirp of monolithic colliding pulse mode-locked diode lasers](#)

Appl. Phys. Lett. **70**, 2514 (1997); 10.1063/1.119086

[Pulseshaping mechanism in collidingpulse modelocked laser diodes](#)

Appl. Phys. Lett. **67**, 3877 (1995); 10.1063/1.115303

[Multiple colliding pulse modelocked operation of a semiconductor laser](#)

Appl. Phys. Lett. **65**, 1894 (1994); 10.1063/1.113002

[Pulse buildup in passively modelocked monolithic quantumwell semiconductor lasers](#)

Appl. Phys. Lett. **63**, 2021 (1993); 10.1063/1.110631

[Transformlimited 1.4 ps optical pulses from a monolithic collidingpulse modelocked quantum well laser](#)

Appl. Phys. Lett. **57**, 759 (1990); 10.1063/1.103413

The logo for the Journal of Applied Physics is displayed on an orange background. The letters 'AIP' are in a large, white, sans-serif font, followed by a vertical bar and the words 'Journal of Applied Physics' in a smaller, white, sans-serif font.

Journal of Applied Physics is pleased to announce **André Anders** as its new Editor-in-Chief

Subpicosecond monolithic colliding-pulse mode-locked multiple quantum well lasers

Y. K. Chen, M. C. Wu, T. Tanbun-Ek, R. A. Logan, and M. A. Chin
AT&T Bell Laboratories, Murray Hill, New Jersey 07974

(Received 7 August 1990; accepted for publication 25 January 1991)

Ultrafast subpicosecond optical pulse generation is achieved by passive colliding-pulse mode locking of monolithic multiple quantum well InGaAsP semiconductor lasers.

Transform-limited optical pulses with durations of 1.1, 0.83, 1.0, and 0.64 ps are achieved at repetition rates of 40, 80, 160, and 350 GHz, respectively, without using any external ac sources.

Generation of short optical pulses with semiconductor laser diodes is important for high bit rate time-division multiplexed communication systems, ultrafast data processing, and picosecond optoelectronic applications. Because the pulse shaping mechanisms are determined by the saturation and recovery time of the gain and absorber sections in mode-locked lasers,¹ it is possible to generate short optical pulses with a repetition rate beyond the relaxation oscillation frequency of the semiconductor laser. The unique optical properties of quantum well semiconductor epitaxial layers such as low dispersion, broad gain spectrum, and the fast saturation and recovery times can well be utilized as the gain and absorber media to generate short mode-locked pulses.²⁻⁴ The use of an integrated waveguide cavity in semiconductor lasers further eliminates the uncontrollable multiple pulse bursts produced by nonperfectly antireflection-coated surfaces in mode-locked lasers with external cavities.⁵⁻⁹ The colliding-pulse mode-locking (CPM) scheme has been widely used to generate short optical pulses in dye lasers, which utilizes the interaction of counterpropagating pulses in the absorber to synchronize, stabilize, and shorten the pulses.¹⁰⁻¹² We reported the generation of transform-limited 1.4 ps pulses from a monolithic active mode-locked CPM multiple quantum well (MQW) semiconductor laser with an external microwave oscillator.¹³ However, a very stable low-noise high-frequency electronic oscillator as well as a fast modulation section are required for the active mode-locking scheme. In this letter, we have implemented a monolithic passive colliding pulse mode-locked laser with a strained multiple quantum well laser structure to generate continuous wave (cw) subpicosecond optical pulses without external microwave sources or any pulse sources. The pulse repetition rate of this passive CPM scheme is only limited by the cavity length and its saturation and recovery characteristics.

The monolithic CPM lasers were fabricated with a 1.5 μm buried heterostructure (BH) GaInAsP graded index separate confinement (GRIN-SCH) lattice-strained MQW structure prepared by a two-step organo-metallic vapor phase epitaxy (OMVPE) growth technique. In the first growth, the lower part of the graded index confining InGaAsP layers were deposited on top of a 2- μm -thick n -InP cladding layer with step-like decreasing band-gap layers of 1.08 μm (25 nm thick), 1.16 μm (25 nm thick),

and 1.25 μm (25 nm thick), and followed by five InGaAs quantum wells (5 nm thick) and 1.25 μm (22.5 nm thick) InGaAsP barriers. The upper graded index InGaAsP confining layers, similar to the lower part, were then grown with increasing band gap, and followed by a 2 μm p -InP cladding layer and a 120 nm p^+ -InGaAsP contact layer (Zn doped to $5 \times 10^{18} \text{ cm}^{-3}$). After the 1- μm -wide continuous waveguide stripes were formed by etching down to the lower n cladding layer with a SiO_2 mask, an iron-doped semi-insulating InP layer was selectively grown around the waveguide strips to provide electrical isolation and optical confinement. Detailed growth conditions and device performance of the MQW lasers were reported in Ref. 14. Standard lithography and wet chemical etching were used to construct the final structure. The schematic diagram of the monolithic passive CPM laser is depicted in Fig. 1. As shown in Fig. 1, the continuous optical waveguide is divided into three sections by segmented p -contact metal stripes. The electrical isolation between contact metals is achieved by removing the heavily doped top p -type contact epitaxial layer with wet chemical etching. Typical resistance across the 10 μm gap is 1 K Ω . The saturable absorber is located in the symmetry center of the linear cavity between two cleaved Fabry-Perot facets. The remaining active cavity sections are connected together and forward biased as the gain sections for the integrated CPM laser.

As in the passive CPM dye lasers, the initial transients proceed to form two counterpropagating pulses at steady state. These two pulses time themselves to collide in the center saturable absorber because minimum energy is lost. Compared to a single pulse traveling in the cavity, the pulse shaping is more effective with the CPM configuration because there are two pulses added coherently to saturate the absorber and only one pulse to saturate the gain section. The transient grating generated by the colliding pulses further reduces the saturation energy of the absorber and limits the necessary spectral bandwidth.^{11,12} Devices of cavity length 2.1, 1.0, 0.534, and 0.25 mm were fabricated to generate optical pulses with repetition rates of 39.2, 80.4, 156, and 350 GHz, respectively. The repetition rate corresponds to one half of the round-trip time between two facets because of the CPM configuration. The length of the saturable absorber is 15 μm for lasers with 0.25 mm cavity length, and is 50 μm for lasers with other cavity lengths.

Typical continuous-wave light-current (L - I) charac-

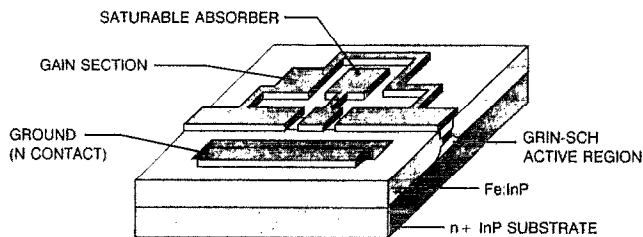


FIG. 1. Schematic diagram of the passive monolithic colliding-phase mode-locked (CPM) quantum well laser.

teristics (solid lines) and photocurrent of the absorber (dashed lines) of a passive CPM laser are shown in Fig. 2 for various absorber voltage, V_{abs} . The cavity length of this CPM laser is 2.1 mm. For uniform current injection (with gain and absorber sections connected together), the L - I curve is almost linear beyond the lasing threshold. Once the saturable absorber is reverse biased, nonlinear L - I curves and photocurrent are observed. The lasing threshold current increases with negative V_{abs} because of the increasing optical loss in the absorber. The saturation of the absorber at high optical power can also be observed in the reverse-biased photocurrent of the MQW absorber. Continuous mode-locked operations are observed when the laser is biased with its output power below 1 mW in Fig. 2. When the output power is beyond 1 mW, self-pulsation starts and the laser is no longer mode locked.

The optical pulse measurements were performed with a noncollinear second-harmonic generating (SHG) autocorrelator. Figures 3 (a)–3(c) shows the measured SHG traces (dots) from the monolithic passive CPM lasers with cavity lengths of 2.1 mm, 1.0 mm, and 534 μm , respectively, and their optical spectra are recorded in Figs. 3(d)–3(f). The zero levels in Figs. 3(a)–3(c) are obtained by blocking the laser beams into the autocorrelator. The extinction ratios are better than 95%, and only a single pulse is observed for each cycle. The repetition rate, f , measured from the SHG trace and the mode spacing, $\delta\lambda$, obtained

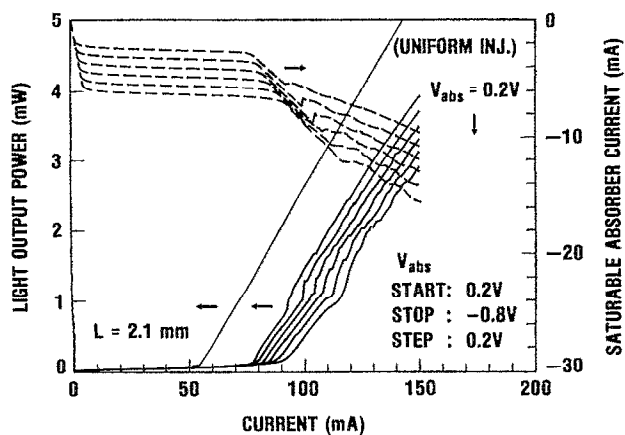


FIG. 2. Continuous-wave output light intensity (solid lines) and photocurrent of the absorber (dashed curves) of a passive CPM laser as a function of the bias current of gain section (I_G) and the voltage on the absorber (V_{abs}). The cavity length is 2.1 mm.

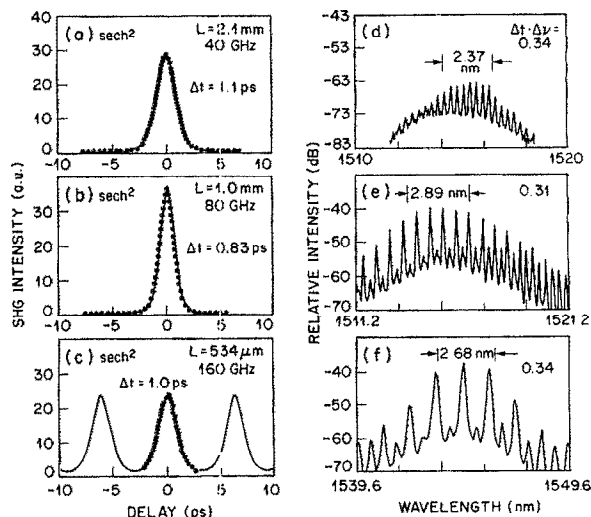


FIG. 3. Second-harmonic generation (SHG) autocorrelation traces of the pulses from passive monolithic CPM lasers of different cavity length: (a) 2.1 mm, (b) 1.0 mm, and (c) 534 μm . The simulated SHG traces (solid curves) agree well with the measured traces (dots) using a hyperbolic-secant pulse shape with transform-limited pulse widths of 1.1, 0.83, and 1.0 ps, respectively. The mode-locked optical spectra are simultaneously recorded in (d), (e), and (f), respectively. Because of the CPM configuration, the corresponding optical pulse repetition rates are 39.2, 80.4, and 156 GHz, respectively. The optical modulation depth is nearly 100%, and only direct-current sources are used.

from the optical spectrum agree well with the round-trip time calculation for the CPM configuration:

$$f = c/nL = c\delta\lambda/\lambda^2, \quad (1)$$

where L is the length of a linear cavity, c is the speed of the light in free space, n is the refractive index of the active waveguide, and λ is the lasing wavelength. Using a hyperbolic-secant pulse waveform, the simulated SHG traces [solid curves in Figs. 3(a)–3(c)] fit very well with the measured data. The full width at half maximum (FWHM) pulse widths of 1.1, 0.83, and 1.0 ps are obtained for CPM lasers with cavity lengths of 2.1 mm, 1.0 mm, and 534 μm , respectively, with very low dc levels of 2.0, 0.3, and 5%. From the measured FWHM spectral widths in Figs. 3(d)–3(f), time-bandwidth products ($\Delta\tau \times \Delta\nu$) are 0.34, 0.31, and 0.34, respectively, which are very close to the transform-limited value of 0.31 for hyperbolic-secant pulses.

By decreasing V_{abs} from +0.6 to -0.05 V, the lasing spectrum can be changed from a dominating single-longitudinal cw lasing mode to a group of double mode-spacing CPM modes as shown in Fig. 4. The corresponding SHG pulse width and extinction ratio are also improved with decreasing V_{abs} . By shortening the cavity length to 250 μm , we are able to obtain subpicosecond pulses at 350 GHz. Because of the large mirror loss in a short cavity laser, the length of the saturable absorber is reduced. Figure 5(a) shows the measured (dots) and calculated (curve) SHG trace of this short-cavity CPM laser.

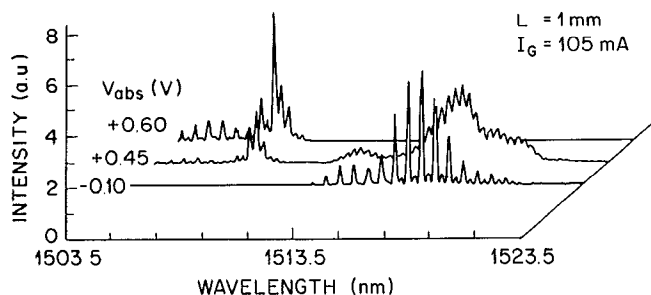


FIG. 4. Influence of the absorber bias voltage (V_{abs}) on the lasing spectra of a 1-mm-long monolithic CPM laser.

It shows a very good fit with a hyperbolic secant pulse shape, and the pulse width is 640 fs with zero dc level in the calculation. The measured FWHM spectral width is 4 nm [Fig. 5(b)] which indicates these optical pulses are

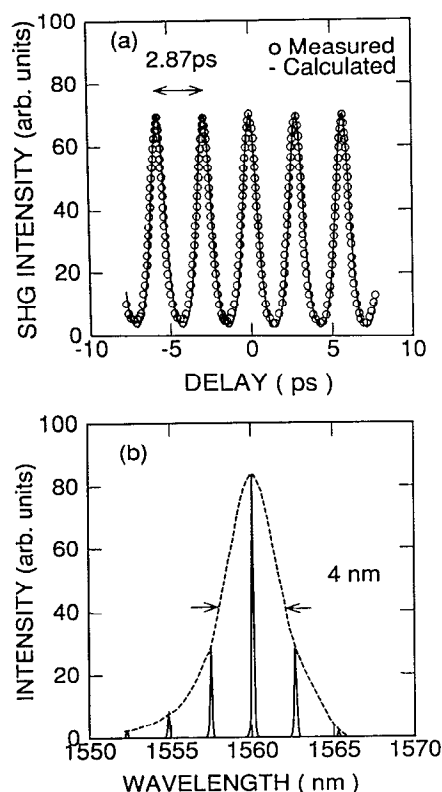


FIG. 5 (a) Measured (dots) and simulated (solid curves) SHG traces of a passive CPM laser with a cavity length of $250 \mu\text{m}$ indicate optical pulses with FWHM pulse width of 640 fs at 350 GHz. A hyperbolic secant pulse shape with zero dc level is used in the simulation. (b) The measured optical spectra of the 350 GHz pulses show a FWHM spectral width of 4 nm. This corresponds to a nearly transform-limited time-bandwidth product of 0.32.

transform limited with a time-bandwidth product of 0.32.

For effective pulse shaping in passive mode-locked lasers, it is necessary for the absorber to saturate faster than the gain.¹ This allows the absorber to sharpen the leading edge of the pulses, while the saturation of gain reduces the trailing edge. The pulse shortening mechanism continues as the pulse makes multiple trips inside the laser cavity. Ultimately, dispersive effects prevent the pulse from becoming narrower. To effectively sharpen optical pulses, the physical length of the saturable absorber should be shorter than the optical pulses. It takes almost 1 ps to traverse a $50 \mu\text{m}$ saturable absorber and two $10 \mu\text{m}$ gaps, or 0.5 ps for the $15\text{-}\mu\text{m}$ -long absorber and gaps. Therefore, the minimum pulse width in this experiment is limited by the physical size of the absorber and the dispersion from the active region. Further optimization in the length and saturation cross section of the absorber together with an integrated low dispersive passive waveguide should reduce the pulse width significantly.

In summary, we have realized the generation of cw subpicosecond optical pulses with passive monolithic colliding pulse mode-locked semiconductor lasers for the first time. Transform-limited subpicosecond pulses are generated at 40, 80, 160, and 350 GHz. The shortest transform-limited pulse width is 640 fs at 350 GHz. This compact cw optical pulse source is very useful for high bit-rate time division multiplex communication system, high-speed optoelectronics, and millimeter wave conversions.

- ¹H. A. Haus and Y. Silberberg, *J. Opt. Soc. Am. B* **2**, 1237 (1985).
- ²For reviews, see W. T. Tsang, in *Semiconductor and Semimetals*, edited by R. Dingle (Academic, Orlando, Florida, 1987), Vol. 24, Chap. 7.
- ³W. H. Knox, R. L. Fork, M. C. Downer, D. A. B. Miller, D. S. Chemla, C. V. Shank, A. C. Gossard, and W. Wiegmann, *Phys. Rev. Lett.* **54**, 1306 (1985); D. S. Chemla and D. A. B. Miller, *J. Opt. Soc. Am. B* **2**, 1155 (1985).
- ⁴Y. Silberberg, P. M. Smith, D. J. Eilenberger, D. A. B. Miller, A. C. Gossard, and W. Wiegmann, *Opt. Lett.* **9**, 507 (1984).
- ⁵K. Y. Lau, *Appl. Phys. Lett.* **52**, 2214 (1988).
- ⁶R. S. Tucker, U. Koren, G. Raybon, C. A. Burrus, B. I. Miller, T. L. Koch, G. Eisenstein, and A. Shahar, *Electron. Lett.* **25**, 622 (1989).
- ⁷P. P. Vasilev and A. B. Sergeev, *Electron. Lett.* **25**, 1050 (1989).
- ⁸P. A. Morton, J. E. Bowers, L. A. Koszi, M. Soler, J. Lopata, and D. P. Witt, *Appl. Phys. Lett.* **56**, 111 (1990).
- ⁹S. Sanders, L. Eng, J. Paslaski, and A. Yariv, *Appl. Phys. Lett.* **56**, 310 (1990).
- ¹⁰R. L. Fork, B. I. Greene, and C. V. Shank, *Appl. Phys. Lett.* **38**, 671 (1981).
- ¹¹E. M. Garmire and A. Yariv, *IEEE J. Quantum. Electron.* **QE-3**, 222 (1967).
- ¹²M. S. Stix and E. P. Ippen, *IEEE J. Quantum. Electron.* **QE-19**, 520 (1983).
- ¹³M. C. Wu, Y. K. Chen, T. Tanbun-Ek, R. A. Logan, M. A. Chin, and G. Raybon, *Appl. Phys. Lett.* **57**, 759 (1990).
- ¹⁴T. Tanbun-Ek, R. A. Logan, H. Temkin, K. Berthold, A. F. J. Levi, and S. N. G. Chu, *Appl. Phys. Lett.* **55**, 2283 (1989).